# Drug efflux pump deficiency and drug target resistance masking in growing bacteria

David Fange[a], Karin Nilsson[a], Tanel Tenson[b], and Måns Ehrenberg[a,1]

[a]Department of Cell and Molecular Biology, Uppsala University, 75124 Uppsala, Sweden; and [b]Institute of Technology, University of Tartu, 50411 Tartu, Estonia

Edited by Peter G. Wolynes, University of California at San Diego, La Jolla, CA, and approved March 24, 2009 (received for review November 12, 2008)

**Recent experiments have shown that drug efflux pump deficiency not only increases the susceptibility of pathogens to antibiotics, but also seems to ''mask'' the effects of mutations, that decrease the affinities of drugs to their intracellular targets, on the growth rates of drug-exposed bacteria. That is, in the presence of drugs, the growth rates of drug-exposed WT and target mutated strains are the same in a drug efflux pump deficient background, but the mutants grow faster than WT in a drug efflux pump proficient background. Here, we explain the mechanism of target resistance masking and show that it occurs in response to drug efflux pump inhibition among pathogens with high-affinity drug binding targets, low cell-membrane drug-permeability and insignificant intracellular drug degradation. We demonstrate that target resistance masking is fundamentally linked to growth-bistability, i.e., the existence of 2 different steady state growth rates for one and the same drug concentration in the growth medium. We speculate that target resistance masking provides a hitherto unknown mechanism for slowing down the evolution of target resistance among pathogens.**

antibiotic resistance | efflux pump inhibition | macrolides

In the years after the Second World War, the wide spread introduction of antibiotics in the treatment of bacterial infections revolutionized medicine and dramatically improved the health condition on a global scale. Now, 60 years later, the ever evolving antibiotic resistance among pathogens has heavily depleted the arsenal of effective antibiotic drugs. We seem to be running out of options, and a return to the pitiful health conditions preceding the Second World War has become an ominous scenario.

Resistance against antibiotic drugs among bacterial pathogens may depend on alterations in intracellular drug targets, reducing their drug affinity or rendering drug binding harmless to their function (1). Bacteria may also evolve enzyme systems degrading the antibiotic drugs (1), or highly efficient drug efflux pumps for rapid export of antibiotics from the bacterial cytoplasm to the growth medium (2, 3).

Increased attention is now being paid to the interplay between drug efflux pump efficiency and inhibition of target function in the cytoplasm. Experiments show that the drug susceptibility of pathogens increases dramatically upon reduction of drug efflux pump efficiency by either genetic manipulation (4, 5) or addition of efflux pump inhibitors (6–9). This feature of drug efflux pump deficiency is intuitively obvious, but recent findings for the ribosome targeting macrolide antibiotic erythromycin suggest the existence of more subtle aspects of the interplay between drug efflux pump efficiency and drug susceptibility. An *Escherichia coli* mutant with an amino acid deletion in protein L22 of the large ribosomal subunit (10, 11), causing reduced affinity of erythromycin to the ribosome (12), displayed reduced susceptibility to erythromycin in relation to a ribosome WT strain in a drug efflux pump proficient but the same susceptibility in a drug efflux pump deficient background (12, 13). These experiments demonstrated how a mutation reducing drug affinity to a vital intracellular target may give a distinct growth advantage to drug exposed bacteria in a drug efflux pump proficient background but virtually no advantage in a drug efflux pump deficient background. That is, the effect of the drug resistance mutation was ''masked'' by drug efflux pump deficiency, despite the fact that the mutation per se seemed not to stimulate drug efflux in the pump proficient situation. Similar ''masking'' results have been reported for L22 and L4 mutations in *Campylobacter jejuni* and *Campylobacter coli* (14) and for a 23S rRNA mutation in *C. coli* (15).

Here, we develop a theory that accounts for the interplay between drug efflux pump efficiency and intracellular drug degradation, on the one hand, and, on the other, mutations that reduce the affinity of drugs to their targets. We show how the reduced drug susceptibility conferred by such target mutations in a drug efflux pump proficient background may be completely lost (masked) in a drug efflux deficient background and define the conditions under which such target resistance masking occurs. The theory does not invoke drug efflux pump stimulation of the target mutations to explain the synergism between pump efflux efficiency and resistance. Instead, it shows resistance masking to emerge when intracellular drug dilution by growth dominates over drug dilution by efflux or degradation. The masking effect is strong for intracellular targets of high drug affinity and high concentration in conjunction with drug efflux pump deficiency, insignificant drug degradation in the cytoplasm, and low cell wall permeability. Accordingly the theory is mandatory for both the design and the interpretation of experiments addressing to the interplay between drug efflux pumps and target resistance.

We also demonstrate that target resistance masking is closely linked to growth-bistability (16), i.e., that a pathogen may grow with either one of 2 different steady state rates in the presence of one and the same concentration of an antibiotic drug in the medium. This finding may have baring on the observation that drug efflux pump deficiency greatly slows down the evolution of target resistance mutations among pathogens (5, 6, 8, 17). Our analysis suggests, in other words, target resistance masking in combination with growth-bistability to be a previously unrecognized cause of delayed drug resistance development among pathogens under drug efflux pump deficient conditions.

## Results

**Synopsis.** First, we set up differential equations for drug transport through the cell envelope and drug binding to intracellular targets of growing bacteria. Second, we derive the conditions under which steady state growth-bistability can arise for bacterial populations exposed to antibiotic drugs. Thirdly, we describe in

Author contributions: M.E. designed research; D.F., K.N., T.T., and M.E. performed research; D.F. contributed new reagents/analytic tools; D.F., K.N., T.T., and M.E. analyzed data; and D.F. and M.E. wrote the paper.

The authors declare no conflict of interest.

This article is a PNAS Direct Submission.

[1]To whom correspondence should be addressed. E-mail: ehrenberg@xray.bmc.uu.se.

This article contains supporting information online at www.pnas.org/cgi/content/full/0811514106/DCSupplemental.

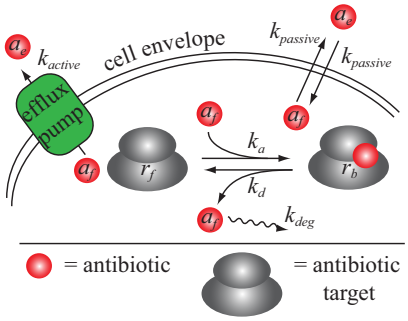


**Fig. 1.** Diagram illustrating drug flows over the cell envelope, drug inactivation and target binding. Drugs enter the cell by passive transport (rate constant $k_{passive}$) and exit by passive transport (rate constant $k_{passive}$), active pumping (rate constant $k_{active}$), drug degradation in the cytoplasm (rate constant $k_{deg}$) and dilution by growth (rate $\mu$, equal to $\mu_0$ in drug free medium). $a_e$ is the external, $a_f$ the free and $a_0$ the total drug concentration in the cell. The total, free and drug-bound target concentrations are $r_0$, $r_f$ and $r_b$, respectively.

detail the steady state aspects of drug resistance masking and its connection with growth-bistability. Finally, we discuss the dynamics of growth inhibition in response to drug addition to or removal from the medium. Detailed derivations and extensions of the theory are given in *SI Appendix*.

**Cell Growth of Drug Exposed Bacteria with Intracellular Drug Targets.** The starting point of our theory, based on the model in Fig. 1, is 2 differential equations that account for drug influx, drug outflux and drug target binding:

$$\frac{dr_f}{dt} = (r_0 - r_f)k_d - a_f r_f k_a - \mu r_f + \mu r_0$$
$$\frac{da_f}{dt} = a_e k_{in} - a_f k_{out} + (r_0 - r_f)k_d - a_f r_f k_a - \mu a_f. \quad [1]$$

Here, $r_0$ and $r_f$ are the total and free intracellular target concentrations, respectively, whereas $a_e$ is the external, and $a_f$ the free intracellular drug concentration. The target-bound drug (or occupied target) concentration, $r_b$, is $r_0 - r_f$, so that the total drug concentration, $a_0$, equals $a_f + r_b$. The rate constants for drug dissociation from and drug association to the target are $k_d$ and $k_a$, respectively. $\mu$ is the growth rate of the bacterial population, equal to $\mu_0$ when $a_e = 0$, whereas $k_{in}$ is the first order rate constant for drug influx from the medium determined by passive transport: $k_{in} = k_{passive}$, where $k_{passive}$ is determined by the cell membrane permeability, $\varepsilon$ ($cm^{-1}$), membrane area, $A$ ($cm^2$), and cell volume V ($cm^3$). The rate constant $k_{out}$ is determined by $k_{passive}$, active transport by drug efflux pumping, $k_{active}$, and intracellular first order drug degradation, $k_{deg}$, so that $k_{out} = k_{passive} + k_{active} + k_{deg}$ (see *SI Appendix* and Fig. S1) for how $k_{out}$ is determined for one (Gram-positive bacteria) and two (Gram-negative bacteria) cell membranes). The inflow per cell volume, $j_{in}$, is equal to $k_{in}a_e$ and the outflow, $j_{out}$, to $k_{out}a_f + \mu a_0$, where the last term is due to drug dilution by growth. To obtain the steady state solution of Eq. **1**, we set the time derivatives on the left hand side to zero and define dimensionless (normalized) variables $\tilde{\mu} = \mu/\mu_0$, $\tilde{j}_{in} = j_{in}/(\mu_0 r_0) = k_{in}a_e/(\mu_0 r_0)$, $\tilde{k}_{out} = k_{out}/\mu_0$, $\tilde{k}_a = k_a r_0/\mu_0$ and $\tilde{k}_d = k_d/\mu_0$ (Table 1). The normalized growth rate $\tilde{\mu}$ is then related to the normalized influx $\tilde{j}_{in}$ through (see *SI Appendix* and Fig. S2)

$$\tilde{j}_{in} = (1 - \tilde{r}_f)\left(\frac{(\tilde{k}_d + \tilde{\mu})(\tilde{k}_{out} + \tilde{\mu})}{\tilde{k}_a \tilde{r}_f} + \tilde{\mu}\right). \quad [2]$$

**Table 1. Summary of model parameters with corresponding normalized parameters**

| Parameter | Description | Normalized parameter |
|---|---|---|
| $r_0$ | Total intracellular target concentration | $\tilde{r}_f = r_f/r_0$ |
| $r_f$ | Free intracellular target concentration | |
| $\mu_0$ | Growth rate* in drug absence | $\tilde{\mu} = \mu/\mu_0$ |
| $\mu$ | Growth rate in drug presence | |
| $a_e$ | Concentration of drug in growth medium | $\tilde{j}_{in} = k_{in}a_e/\mu_0 r_0$ |
| $k_{in}$† | Rate constant for drug influx | |
| $k_{out}$‡ | Sum of rate constant for drug efflux/degradation | $\tilde{k}_{out} = k_{out}/\mu_0$ |
| $k_d$ | Rate constant for drug dissociation | $\tilde{k}_d = k_d/\mu_0$ |
| $k_a$ | Rate constant for drug association | $\tilde{k}_a = k_a r_0/\mu_0$ |

*Growth rate = $\log_2$/(generation time).
†$k_{in} = k_{passive}$.
‡$k_{out} = k_{passive} + k_{active} + k_{deg}$.

**Drug Induced Growth-Bistability.** Steady state growth-bistability for drug-exposed bacterial populations was discussed in the special case of equilibration between free and target-bound drug in the bacterial cytoplasm (16), and here we generalize the treatment by taking also nonequilibrated scenarios into account. When the normalized growth rate, $\tilde{\mu}$, increases monotonically with the fraction, $\tilde{r}_f = r_f/r_0$, of drug free targets, there is an inverse function, $\tilde{r}_f = \tilde{r}_f(\tilde{\mu})$, relating $\tilde{j}_{in}$ to $\tilde{\mu}$ in Eq. **2**:

$$\tilde{j}_{in} = (1 - \tilde{r}_f(\tilde{\mu}))\left(\frac{(\tilde{k}_d + \tilde{\mu})(\tilde{k}_{out} + \tilde{\mu})}{\tilde{k}_a \tilde{r}_f(\tilde{\mu})} + \tilde{\mu}\right). \quad [3]$$

When $\tilde{\mu}$ is approximated by the drug-free fraction of target molecules, $\tilde{r}_f$, Eq. **3** simplifies to

$$\tilde{j}_{in} = (1 - \tilde{\mu})\left(\frac{(\tilde{k}_d + \tilde{\mu})}{\tilde{k}_a} \cdot \frac{(\tilde{k}_{out} + \tilde{\mu})}{\tilde{\mu}} + \tilde{\mu}\right). \quad [4]$$

In Eq. **4**, when $\tilde{k}_d \gg \tilde{\mu}$, free and target-bound drugs are equilibrated and the target part of the growth inhibition (left factor in first term of the big parenthesis) equals $K_D/r_0$, where $K_D = k_d/k_a$ (16). When $\tilde{k}_d \ll \tilde{\mu}$, this factor is independent of $\tilde{k}_d$ and equals $\mu/(k_a r_0)$. For one and the same value of $a_e$ or, equivalently, $\tilde{j}_{in}$, there may be 2 stable steady state values of $\tilde{\mu}$ in Eqs. **3** and **4**, as illustrated in Fig. 2*A* for the $\tilde{\mu} = \tilde{r}_f$ case. The possibility of growth-bistability depends on the normalized rate constants for association to ($\tilde{k}_a$) and dissociation from ($\tilde{k}_d$) the target and on the rate constant $\tilde{k}_{out}$ (Eq. **S11**, Fig. S3, and Fig. 2*B*). The analytical results below are derived for the $\tilde{\mu} = \tilde{r}_f$ case, but the inhibitory action of a drug may deviate from this linear dependence of $\tilde{\mu}$ on $\tilde{r}_f$. For instance, the inhibitory action of erythromycin on ribosomes and growth rate is quite complex (12) and intracellular control systems may respond in different ways to target inhibition. However, we have found that the existence of growth-bistability is robust to variation in the exact functional relation between $\tilde{\mu}$ and $\tilde{r}_f$, as exemplified by a weaker ($\tilde{\mu} = \tilde{r}_f^{1/2}$ in Eq. **3**) and a stronger ($\tilde{\mu} = \tilde{r}_f^2$ in Eq. **3**) dependence of the growth rate on the fraction of free target, compared with the case in Eq. **4** (see *SI Appendix* and below).

The plots in Fig. 2*B* reveal growth-bistability to be favored by inefficient drug transport out from the cell and small rate of drug degradation (small $\tilde{k}_{out}$), large drug affinity to the target and large target concentration (large $\tilde{k}_a$ and small $\tilde{k}_d$). All these characteristics reflect the ultimate cause of growth-bistability,

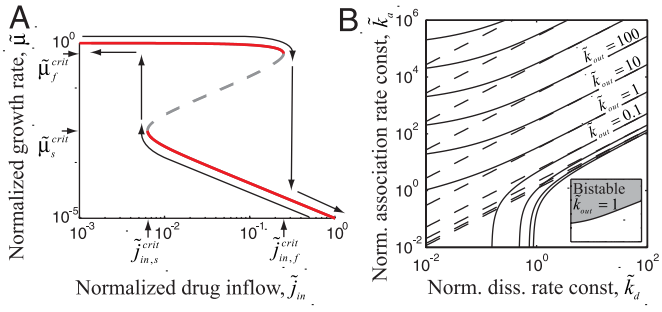


**Fig. 2.** Growth bistability and the conditions under which it occurs. (*A*) The growth rate, $\tilde{\mu}$ (*y* axis), is plotted as a function of the drug influx, $\tilde{j}_{in}$ (*x* axis), with $\tilde{k}_a = 10^6$, $\tilde{k}_{out} = 10$, and $\tilde{k}_d = 1$. Upper red curve: when $\tilde{j}_{in}$ increases from zero to $\tilde{j}_{in} = \tilde{j}^{crit}_{in,f} = 1/4$, then $\tilde{\mu}$, approximated by $(1 + \sqrt{1 - 4\tilde{j}_{in}})/2$, decreases from 1.0 to ½, at which point the fast growth regime disappears. Lower red curve: when $\tilde{j}_{in}$ decreases from high values to $\tilde{j}_{in} = \tilde{j}^{crit}_{in,s} = 2\sqrt{\tilde{k}_d\tilde{k}_{out}/\tilde{k}_a}$, then $\tilde{\mu}$, approximated by $\tilde{j}_{in}(1 - \sqrt{1 - 4\tilde{k}_d\tilde{k}_{out}/(\tilde{j}^2_{in}\tilde{k}_a)})/2$, increases to $\sqrt{\tilde{k}_d\tilde{k}_{out}/\tilde{k}_a}$, at which point the slow growth regime disappears (see Table 1 for parameter definitions). In gray: steady-state growth rate according to Eq. **4**, where the solid curves (partially hidden by approximation in red) represent stable steady-states and the dashed curve represents unstable steady-states. (*B*) The association, $\tilde{k}_a$ (*y* axis), and dissociation, $\tilde{k}_d$ (*x* axis), rate constants for drug-target interaction at which growth-bistability can arise for different values of the drug efflux rate constant, $\tilde{k}_{out}$. Growth-bistability is confined to areas ''northwest'' of the solid curves, illustrated by the shaded area in the insert. For $\tilde{k}_d$ values much >1, all curves are straight lines, corresponding to equilibration between free and target-bound drug (16). Dashed lines indicate the result of an equilibrium assumption, in regions where the equilibrium condition is not valid. The inequality defining the northwest region is given by Eq. **S11** in *SI Appendix*.

namely that in the fast growth regime, where the growth rate, $\tilde{\mu}$, decreases from 1 to ≈1/2 (see Fig. 2*A* and below), the major pathway for reduction of the total intracellular drug concentration is "dilution-by-growth," rather than drug efflux and/or drug degradation. The "dilution-by-growth" condition is defined by the inequality:

$$\frac{(\tilde{k}_d + \tilde{\mu})(\tilde{k}_{out} + \tilde{\mu})}{\tilde{k}_a\tilde{\mu}} \ll \tilde{\mu}. \qquad [5]$$

The right hand side is the normalized rate of dilution by growth, operating on the total intracellular drug concentration, whereas the left hand side describes the out flow and degradation ($\tilde{k}_{out}$) operating on the fraction of intracellular drug concentration that is free, as mainly determined by $\tilde{k}_d$ and $\tilde{k}_a$. When the inequality in Eq. **5** is satisfied, it follows from Eq. **4** that $\tilde{\mu}$ is approximated by (*SI Appendix*, Eq. **S16**)

$$\tilde{\mu} = \frac{1}{2}\left(1 + \sqrt{1 - 4\tilde{j}_{in}}\right). \qquad [6]$$

Accordingly, $\tilde{\mu}$ decreases from 1.0 down to 1/2, as $\tilde{j}_{in}$ increases from zero in the absence of drug in the medium to its critical value $\tilde{j}^{crit}_{in,f} = 1/4$ (Fig. 2*A*). When $\tilde{j}_{in}$ increases above 1/4, the real-valued solution to Eq. **6** disappears as the system exits the fast growth regime. As a result, $\tilde{\mu}$ decreases abruptly to a value much <1.0 and the intracellular drug concentration increases dramatically. It follows from Eq. **4** that in the slow growth regime, $\tilde{\mu}$ is approximated by (*SI Appendix*, Eq. **S18**)

$$\tilde{\mu} = \frac{\tilde{j}_{in}}{2}\left(1 - \sqrt{1 - \frac{4\tilde{k}_d\tilde{k}_{out}}{\tilde{j}^2_{in}\tilde{k}_a}}\right). \qquad [7]$$

For large values of $\tilde{j}_{in}$, Eq. **7** can be Taylor expanded to

$$\tilde{\mu} = \frac{\tilde{k}_d\tilde{k}_{out}}{\tilde{j}_{in}\tilde{k}_a}. \qquad [8]$$

This means that when the system leaves the fast and enters the slow growth regime, $\tilde{\mu}$ drops "vertically" from ½ to

$$\frac{4\tilde{k}_d\tilde{k}_{out}}{\tilde{k}_a} = \frac{4K_D\tilde{k}_{out}}{r_0}$$

and is thereafter proportional to the dissociation constant, $K_D$, for drug binding to the target.

The slow growth regime is stable for decreasing values of $\tilde{j}_{in}$ until the slow growth critical point (Fig. 2*A*): $\tilde{j}^{crit}_{in,s} = 2\sqrt{\tilde{k}_d\tilde{k}_{out}/\tilde{k}_a}$, where $\tilde{\mu} = \sqrt{\tilde{k}_d\tilde{k}_{out}/\tilde{k}_a}$. When $\tilde{j}_{in}$ decreases further, the real-valued solution to Eq. **7** disappears and $\tilde{\mu}$ returns to the fast growth regime. It follows that the growth-bistable regime is "boxed in" by the following inequalities

$$2\sqrt{\tilde{k}_d\tilde{k}_{out}/\tilde{k}_a} = \tilde{j}^{crit}_{in\,s} < \tilde{j}_{in} < \tilde{j}^{crit}_{inf} = 1/4. \qquad [9]$$

Note that according to Eq. **6** the fast growth regime behavior of the cell population does not depend on the association and dissociation rate constants for drug-target interactions. One consequence of this is that as long as the inequality in Eq. **5** holds, target resistance alterations decreasing the association rate constant, $k_a$, or increasing the dissociation rate constant, $k_d$, do not affect the minimal inhibitory drug concentration (MIC value, see next section). This means, in other words, that the ultimate cause of growth-bistability is also the ultimate cause of "masking" of the growth effects of target resistance mutations in the fast growth regime as described in the next section.

**Drug Efflux Deficiency Masking of Target Resistance Mutations.** In this section, we inspect how target resistance mutations that decrease $k_a$ values and increase $k_d$ values affect pathogen growth in the presence of antibiotic drugs under conditions of drug efflux proficiency and deficiency. For this, we use Eq. **4** to compute the growth rate at varying external drug concentration for bacterial WT and resistance mutated populations. In one test-case, there is a 100-fold or a 10,000-fold larger $k_d$ value for the target-mutated than for the WT pathogen. The parameters are chosen so that the target-WT pathogen displays growth-bistability in the drug-efflux deficient but not the drug-efflux proficient background, and the result is shown in Fig. 3*A*.

As expected, drug-efflux deficiency promotes greatly increased drug susceptibility of all 3 strains (Fig. 3*A*). We can also observe that the $MIC_{50\%}$ values, here defined as the normalized minimal inhibitory drug concentration, $a_e/r_0$, conferring at least 50% reduction of growth rate, increase with increasing drug efflux (see Fig. 3*B*). Note that the normalized drug concentration, $a_e/r_0$, is proportional to the drug inflow (Table 1) and that in Fig. 3*B* we have assumed that $\tilde{k}_{in} = k_{in}/\mu_0 = 1$, so that the normalized drug inflow, $\tilde{j}_{in}$, becomes $\tilde{j}_{in} = \tilde{k}_{in}a_e/r_0 = a_e/r_0$. More unexpected, the normalized $MIC_{50\%}$ values for WT and mutants are identical ($MIC_{50\%} \approx 0.25$) under the drug-efflux deficient condition but distinct under the drug-efflux proficient condition (Fig. 3*A*, intersections with upper horizontal dotted line where $\tilde{\mu} = 0.5$). In fact, the $MIC_{50\%}$ values remain identical as the drug-efflux rate constant ($\tilde{k}_{out}$) increases from 10, defining drug-efflux deficiency in Fig. 3*A*, up to 100 (Fig. 3*B*), after which the $MIC_{50\%}$ value of the lowest affinity mutant increases (green curve in Fig. 3*B*), whereas the $MIC_{50\%}$ values of the WT and the middle affinity mutant remain at 0.25. The latter 2 $MIC_{50\%}$ values do not visibly diverge until the $\tilde{k}_{out}$ value supersedes 10,000 (blue and black curves in Fig. 3*B*). The underlying reason for this behavior can be traced to the inequality in Eq. **5** as

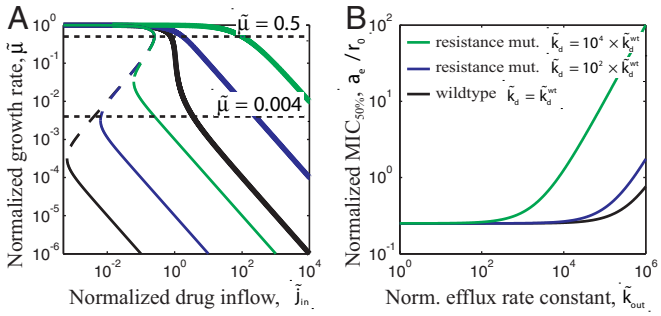


**Fig. 3.** Drug target resistance masking and its dependence on low drug-efflux pump efficiency. (*A*) Normalized steady state growth rate ($\tilde{\mu}$, *y* axis) as function of drug normalized influx ($\tilde{j}_{in}$, *x* axis) into the bacterial cells for drug-efflux proficient (thick lines) and deficient (thin lines) cells for target WT (black) and target resistance mutated (blue, 100 × WT dissociation rate constant) and (green, 10,000 × WT dissociation rate constant) strains. For the target WT strain we use $k_a = 10^6$, $k_d = 0.01$ and we use $k_{out} = 10$ in the drug-efflux deficient and $k_{out} = 10^6$ in the drug-efflux proficient background (see Table 1 for parameter definitions). Solid and dashed lines are stable and unstable steady-states, respectively. The upper and lower dotted horizontal lines indicate normalized growth rates of 0.5 and 0.004, respectively. (*B*) Normalized minimal inhibitory concentration at 50% reduction of growth rate ($MIC_{50\%} = a_e/r_0$, *y* axis) as function of the drug efflux rate constant ($k_{out}$, *x* axis) for the WT and resistance mutated strains as in A with the same color code. Here, it is assumed that $k_{in}/\mu_0 = 1$, so that $\tilde{j}_{in} = a_e/r_0$.

illustrated in Fig. 3*B*: As long the inequality is fulfilled for both WT and resistance mutants, they all display growth-bistability with identical drug inhibition patterns in their fast growth regime. Divergent inhibition patterns and distinct $MIC_{50\%}$ values appear when the inequality in Eq. **5** is violated by large changes in $k_a$ or $k_d$ values or by greatly increased drug-efflux pump efficiency (Fig. 3*B*). Accordingly, "masking" of target resistance mutations and growth-bistability are but two sides of the same underlying phenomenon. Furthermore, under the drug-efflux deficient condition in Fig. 3*A*, also MIC values defined as the normalized external drug concentration ($a_e/r_0$) at which the fractional growth rate, $\tilde{\mu}$, has been reduced to <0.4% ($MIC_{0.4\%}$) are identical for target WT and target mutants and the same as the $MIC_{50\%}$ values (Fig. 3*A*, between upper and lower horizontal dotted line). This reflects the "vertical" drop in growth rate as the strains leave the fast growth regime (Eq. **6**) and transit through the "no man's land" without stationary solution down to its slow growth regime (Eq. **8** and Fig. 3*A*).

In the slow growth regime, in contrast, the inequality in Eq. **5** is always violated because of small $\tilde{\mu}$ values and here the target affinity differences between mutant and WT strains are fully expressed as shown in Eq. **8** and illustrated by the lower curves in Fig. 3*A*. This means, in summary, that WT and mutant strains are equally inhibited by antibiotic drugs in the fast growth regime, but in the slow growth regime they are inhibited in proportion to the affinity of their target to the antibiotic drug.

When the relation $\tilde{\mu} = \tilde{r}_f$ is replaced by the power law $\tilde{\mu} = \tilde{r}_f^{1/n}$, where *n* values >1 reflect a weak and *n* values <1 reflect a strong dependence of the growth rate on the fraction of free targets, the main results regarding growth-bistability and target resistance masking remain unaltered. For instance, both growth-bistability (*SI Appendix* and Fig. S4) and target resistance masking are similar for $n = 2$, $n = 1$ and $n = 1/2$ (Fig. 3*A*, Fig. S4), but the parameter regions allowing for growth-bistability (Fig. 2*B*) are somewhat different in the 3 cases. In the slow growth regime, the growth rate decreases in proportion $1/\tilde{j}_{in}^{1/n}$ (See *SI Appendix*, Eq. **S20**) and thus more rapidly for small than for large *n* values. One consequence of this is that the growth rate drops "vertically" to a much lower value when $\tilde{j}_{in}$ increases beyond $\tilde{j}_{in,f}^{crit}$ for small than for large values of *n* (see Fig. 3*A* and Fig. S4).

**Dynamics of Growth Inhibition.** The time for bacterial growth to reach steady state after drug addition to or drug removal from the growth medium is in general much longer for drug efflux pump deficient than for drug efflux pump proficient cells, as described in detail in *SI Appendix*. Strikingly long adjustment times are observed when drug efflux pump deficient strains, displaying target resistance masking and growth-bistability, are exposed to concentrations close to the "critical" points at which the cell population moves from the fast to the slow growth regime or moves from the slow to the fast growth regime (Fig. S5 *A* and C). Accordingly, such dynamic measurements can be used to reject or corroborate the existence of target resistance masking and growth-bistability according to the mechanism proposed in the present work. To illustrate, we compare the approach to the steady state of the drug-efflux deficient strains in Fig. 3, when they first grow in the absence of antibiotics and then are rapidly exposed to the drug at a normalized drug concentration ($a_e/r_0$) of 0.3, just above the critical concentration of 0.25 at which the fast growth regime disappears (Fig. S5*A*). The growth rates of all 3 strains decrease similarly and very slowly in the fast growth regime, until they decrease sharply at the same point in time to their different values in the slow growth regime. Similarly, very slow transition times are observed for cell populations in the slow growth regime that are exposed to a drug concentration just below the critical point at which the slow-to-fast transition occurs (Fig. S6*E* and Fig. S7).

## Discussion

Mutations that reduce the affinity of antibiotic drugs to intracellular targets are common among pathogens and they are known to reduce the drug susceptibility and thus increase the MIC value of bacterial mutants. Here, we have shown that affinity reducing target mutations, which lead to reduced antibiotic susceptibility in the presence of efficient drug efflux pumps and/or drug inactivation in the cytoplasm, may have no effect on the drug susceptibility when the efflux pumps are inhibited or absent and intracellular drug inactivation is negligible. The growth advantage for drug exposed pathogens conferred by reduced target affinity may, in other words, be conditional on the presence of rapid drug efflux from the cytoplasm or efficient drug inactivation. The disappearance of this growth advantage of a drug exposed mutant in relation to WT, due to drug efflux pump and drug inactivation deficiency, we have named "target resistance masking."

Questions we have addressed are: How can the same drug efflux reduction in WT and mutant eliminate the relative growth advantage of the drug-exposed mutant? Under what condition does target resistance masking occur? Is target resistance masking medically relevant?

**What Is the Working Principle of Target Resistance Masking?** To get an intuitive understanding of target resistance masking, we focus on scenarios where the degree of growth inhibition by the drug is determined by the fraction of drug-bound targets (see Fig. 1). When the target has high affinity to the drug and/or is present at high concentration in the cytoplasm, virtually all intracellular drug molecules are target bound as long as their total concentration is smaller than that of the target. The inflow of drug molecules from the external medium to the cytoplasm is determined by passive transport over the cell membrane(s). It depends on the external drug concentration and the drug permeability of the cell membrane(s) and is the same for WT and target resistance mutants. The out flow is determined by passive transport of drugs by diffusion over the cell membrane(s), by pump-mediated active transport through the cell membrane(s), by enzymatic drug degradation and, finally, by dilution-by-growth. The flows in the first 3 pathways for drug reduction in the cell are proportional to the free concentration of the drug in

the cytoplasm, whereas the last flow is proportional to the total drug concentration and the growth rate $\mu$ (Fig. 1). For one and the same total drug concentration in the cytoplasm, the free intracellular drug concentration will be higher for the target mutant than for the WT. In drug efflux pump proficient cells, where drugs are mainly removed by efflux over the cell membrane(s) with a rate proportional to the free drug concentration, reduced target affinity to the drug will lead to larger efflux and thus to decreased total drug concentration in the cytoplasm. This means that mutants with reduced target affinity to drugs will have smaller drug susceptibility and higher MIC values than WT. What about drug efflux pump deficient strains with small cell membrane permeability? Here, the drug outflow through the cell membrane(s) may be so small that drug efflux is dominated by drug dilution by growth, rather than by transport over the cell membrane(s). Then, for the same growth rate, the outflow will be virtually the same for WT and target mutant. Because also the drug inflows are equal for WT and mutant, they will have virtually the same total drug concentration in the cytoplasm, the same fraction of free target and thus the same drug susceptibility and growth rate. Accordingly, the target affinity difference is functionally "masked," as long as the growth rate remains sufficiently high to maintain dilution-by-growth as the dominant pathway for drug reduction in both target WT and mutant. Target resistance masking requires low cell membrane permeability, high target affinity to drug and high intracellular target concentration as defined by the inequality in Eq. **5**. From this follows that target resistance masking may occur for relatively high growth rates, but what happens when the external drug concentration increases further so that growth inhibition becomes more severe? To answer this question, we need to take into account another finding of the present work, namely that target resistance masking is fundamentally linked to growth-bistability.

That is, when the dominant pathway for drug reduction in the cytoplasm is dilution by growth, the cell population also displays growth-bistability and hysteresis with 2 possible growth rates for one and the same external drug concentration (Fig. 2*A*). When the external drug concentration exceeds a critical value at which the growth rate is 50% inhibited (Eq. **6**), the fast growth regime disappears and the growth rate drops to a very small value (Eq. **8**), as the cell population enters the slow growth regime (Fig. 2*A*). Here, the growth rate is so small that drug diffusion over the membrane(s) is the dominant pathway for drug reduction in the cell and, thus, the target affinity difference between WT and mutant is fully expressed as a growth rate difference (Eq. **8** and Fig. 3*A*).

One may ask whether the condition for target resistance masking and growth-bistability is too stringent to be relevant for "real" bacterial pathogens. To inspect this, and to further illustrate the fundamental connection between growth-bistability and target resistance masking, we discuss a simple example (see *SI Appendix* and Fig. S8). In this, we use what we deem as realistic values for growth rate, drug permeability, drug affinities to target and target concentration. The experimental conditions mimic those of recently published observations (12, 13), that will be discussed in the next section.

**Experimental Evidence for Resistance Masking in Bacteria.** The bacterial ribosome is a common target for clinically relevant antibiotic drugs (18, 19), and its intracellular concentration is high, i.e., ≈20 $\mu$M in *E. coli* (20). Macrolides and ketolides bind with high affinity to the 23S rRNA of the 50S ribosomal subunit (21). Quantitative estimates of cell wall permeability for these drugs are missing, but it is expected to be small, because they diffuse slowly through the phospholipid bilayer, because of their hydrophilic character, and slowly through the porins, because of their large size (22).

MIC values for various macrolides and ketolides were recorded for nonisogenic WT and 23S rRNA mutated (A2057G) strains of *C. coli* (*C. coli*) with an intact and a *cmeB* deleted CmeABC efflux pump (15). In the case of the macrolide erythromycin, the A2057G mutation conferred an ≈250-fold higher MIC value than WT in the efflux pump proficient background but only an ≈8-fold higher MIC value in the drug efflux pump deficient background. In the case of the ketolide telitromycin, the A2057G mutation conferred an ≈6-fold higher MIC value in the drug efflux proficient and virtually no MIC value increase in the drug efflux deficient background. The first observation is in line with partial masking of target resistance, whereas the second is in line with complete masking of target resistance by the drug efflux pump deficiency (compare with Fig. S8).

Spontaneous macrolide-resistance mutations in ribosomal proteins L4 and L22 were obtained by plating C. *jejuni* and *C. coli* in the presence of erythromycin and tylosin (14). MIC values were recorded for the 2 macrolides in isogenic drug efflux proficient and deficient (*cmeB*-deleted) strains containing either one of the L4 and L22 mutations. In the *C. coli* strains, the target WT had an erythromycin MIC value ($\mu$g/mL) of 4 in the drug efflux proficient and 0.25 in the drug efflux deficient background, whereas the L22 mutant had a MIC value of 256, i.e., 64 times larger than WT, in the drug efflux proficient and 0.25, i.e., the same as WT, in the drug efflux deficient background. In the tylosin case, the L22 and L4 mutations conferred greatly enhanced and varying MIC values for both the *C. coli* and *C. jejuni* strains in the drug efflux pump efficient but invariably the same MIC value of 0.5 for WT and target mutants in the drug efflux deficient background. Also these striking observations are compatible with complete target resistance masking (Fig. S8), but the experiments are semiquantitative and lack biochemical data on target affinity, as in the erythromycin case in the previous paragraph.

Very recently, it was demonstrated by more quantitative experiments that an amino acid deletion in protein L22 of an *E. coli* strain reduced its susceptibility to erythromycin in a drug efflux proficient, but not in a drug efflux deficient (Δ*tolC*) background (12, 13). Interestingly, when the experiment was carried out in Δ*acrB* strains, retaining residual drug efflux pump activity, the L22 mutation conferred a susceptibility reduction that was significant but much smaller than the reduction seen in the drug efflux pump proficient background (12, 13). Biochemical experiments showed that the L22 alteration reduced ≈50-fold the rate constant for erythromycin binding to and ≈10-fold the rate constant for erythromycin dissociation from the ribosome, corresponding to an ≈5-fold overall affinity loss (12). It was, furthermore, shown by modeling, taking the complex mode of action of erythromycin into account (12), that the erythromycin affinity loss due to the L22 alteration could account for the erythromycin induced growth inhibition observed in the drug efflux proficient, the Δ*acrB* and Δ *tolC* backgrounds (12). At the same time, the L22 mutation did not stimulate drug efflux by up-regulation of the expression of existing pump protein genes in the drug efflux proficient background (13), which led Moore and Sauer to the ad hoc proposition that the L22 mutation favored ribosomal synthesis of unfolded proteins, thereby causing a change in the cell wall permeability.

**Target Resistance Masking and the Evolution of Drug Resistance.** There are several reports in the literature that drug efflux pump deficiency greatly slows down the evolution of drug target resistance among pathogens exposed to antibiotics (e.g., refs. 4, 6, 7, and 17). The rapid evolution of drug resistance among bacterial pathogens is today a major clinical problem (23, 24), and the reports on slow drug resistance evolution are important in that they suggest a combination of efflux pump inhibitory

drugs and growth inhibitory drugs as a future strategy for effective treatment of bacterial disease with minimal risk of target resistance development (6). One reason for the slowing down of target resistance emergence by drug efflux pump deficiency may simply be the greatly enhanced drug susceptibility that arises by drug efflux inhibition (6). Another, that the growth rate recovery time after drug removal is much longer under conditions of drug efflux deficiency than proficiency (Fig. S5 *B* and *D*). In the present work, we have shown that when drug efflux pump deficiency is associated with target resistance masking and growth-bistability, there are 2 regimes with greatly separated growth rates (Fig. 2*A*). In the fast growth regime, there is no difference between WT and all those mutants for which growth-bistability is retained (Fig. 3*A*). Here, there is no fitness advantage for the mutant in relation to the WT during growth at any concentration of the growth inhibitory drug and thus no possibility for the mutant to take over the population. In the slow growth regime, in contrast, target resistance mutations are fully expressed as fitness gains in relation to WT (Fig. 3*A*), but here the growth rates of both WT and mutants may be too slow to allow survival of either strain when attacked by the immune system. There may, in other words, be clinically important scenarios in which target resistance masking and growth-bistability contribute to the containment of drug resistance evolution. These may be further analyzed with population genetic approaches in conjunction with the present findings.

**ACKNOWLEDGMENTS.** We thank Drs. Johan Elf and Martin Lovmar for valuable comments on the manuscript. This work was supported by the Swedish Medical Research Council (M.E.) and the European Regional Development Fund through the Center of Excellence in Chemical Biology (T.T.).

1. Walsh C (2000) Molecular mechanisms that confer antibacterial drug resistance. *Nature* 406:775–781.
2. Lomovskaya O, Zgurskaya HI, Totrov M, Watkins WJ (2007) Waltzing transporters and 'the dance macabre' between humans and bacteria. *Nat Rev Drug Discovery* 6:56–65.
3. Piddock LJ (2006) Multidrug-resistance efflux pumps - not just for resistance. *Nat Rev Microbiol* 4:629–636.
4. Lomovskaya O, et al. (1999) Use of a genetic approach to evaluate the consequences of inhibition of efflux pumps in Pseudomonas aeruginosa. *Antimicrob Agents Chemother* 43:1340–1346.
5. Oethinger M, Kern WV, Jellen-Ritter AS, McMurry LM, Levy SB (2000) Ineffectiveness of topoisomerase mutations in mediating clinically significant fluoroquinolone resistance in Escherichia coli in the absence of the AcrAB efflux pump. *Antimicrob Agents Chemother* 44:10–13.
6. Lomovskaya O, et al. (2001) Identification and characterization of inhibitors of multidrug resistance efflux pumps in Pseudomonas aeruginosa: Novel agents for combination therapy. *Antimicrob Agents Chemother* 45:105–116.
7. Markham PN (1999) Inhibition of the emergence of ciprofloxacin resistance in Streptococcus pneumoniae by the multidrug efflux inhibitor reserpine. *Antimicrob Agents Chemother* 43:988–989.
8. Markham PN, Neyfakh AA (1996) Inhibition of the multidrug transporter NorA prevents emergence of norfloxacin resistance in Staphylococcus aureus. *Antimicrob Agents Chemother* 40:2673–2674.
9. Markham PN, Westhaus E, Klyachko K, Johnson ME, Neyfakh AA (1999) Multiple novel inhibitors of the NorA multidrug transporter of Staphylococcus aureus. *Antimicrob Agents Chemother* 43:2404–2408.
10. Apirion D (1967) Three genes that affect Escherichia coli ribosomes. *J Mol Biol* 30:255–275.
11. Wittmann HG, et al. (1973) Biochemical and genetic studies on two different types of erythromycin resistant mutants of Escherichia coli with altered ribosomal proteins. *Mol Gen Genet* 127:175–189.
12. Lovmar M, et al. (2009) Kinetic coupling between target binding and efflux pump efficiency—The case of erythromycin resistance. *EMBO J* 28:736–744.
13. Moore SD, Sauer RT (2008) Revisiting the mechanism of macrolide-antibiotic resistance mediated by ribosomal protein L22. *Proc Natl Acad Sci USA* 105:18261–18266.
14. Cagliero C, Mouline C, Cloeckaert A, Payot S (2006) Synergy between efflux pump CmeABC and modifications in ribosomal proteins L4 and L22 in conferring macrolide resistance in Campylobacter jejuni and Campylobacter coli. *Antimicrob Agents Chemother* 50:3893–3896.
15. Cagliero C, Mouline C, Payot S, Cloeckaert A (2005) Involvement of the CmeABC efflux pump in the macrolide resistance of Campylobacter coli. *J Antimicrob Chemother* 56:948–950.
16. Elf J, Nilsson K, Tenson T, Ehrenberg M (2006) Bistable bacterial growth rate in response to antibiotics with low membrane permeability. *Phys Rev Lett* 97:258104.
17. Ricci V, Tzakas P, Buckley A, Piddock LJ (2006) Ciprofloxacin-resistant Salmonella enterica serovar Typhimurium strains are difficult to select in the absence of AcrB and TolC. *Antimicrob Agents Chemother* 50:38–42.
18. Poehlsgaard J, Douthwaite S (2005) The bacterial ribosome as a target for antibiotics. *Nat Rev Microbiol* 3:870–881.
19. Tenson T, Mankin A (2006) Antibiotics and the ribosome. *Mol Microbiol* 59:1664–1677.
20. Bremer, H. & Dennis, P (1996) in *Escherichia coli and Salmonella: Cellular and Molecular Biology*, ed Neidhardt FC (ASM, Washington, DC).
21. Douthwaite S, Hansen LH, Mauvais P (2000) Macrolide-ketolide inhibition of MLS-resistant ribosomes is improved by alternative drug interaction with domain II of 23S rRNA. *Mol Microbiol* 36:183–193.
22. Nikaido, H (2003) Molecular basis of bacterial outer membrane permeability revisited. *Microbiol Mol Biol Rev* 67:593–656.
23. Furuya EY, Lowy FD (2006) Antimicrobial-resistant bacteria in the community setting. *Nat Rev Microbiol* 4:36–45.
24. Martinez JL, Baquero F, Andersson DI (2007) Predicting antibiotic resistance. *Nat Rev Microbiol* 5:958–965.